

Design and Development of LLC Resonant Converter for EV Charging

MTP Stage 1 report

Submitted by
Aditya Kumar
(Roll no. 24M1355)

Under the guidance of
Prof. Siddavatam Ravi Prakash Reddy



October 2025

Department of Energy Science and Engineering
Indian Institute of Technology Bombay

Abstract

With the rapid growth of electric vehicles (EVs), the need for efficient, compact, and reliable power conversion systems in EV chargers has become critical. Resonant converters, known for their soft-switching capabilities and high efficiency, are particularly well-suited for such applications. This project focuses on the comparative study and design of resonant converter topologies—specifically the Series Resonant Converter (SRC) and Parallel Resonant Converter (PRC)—as a foundational step toward the eventual development of an LLC resonant converter for EV charging. Key parameters such as resonant tank design, determining the voltage gain using First Harmonic Approximation (FHA) technique, voltage gain characteristics, and zero-voltage switching (ZVS) conditions are analyzed. Simulation models are also developed to validate the behavior of SRC and PRC under varying load conditions and switching frequencies. In this report a review on LLC resonant converter is presented and simulation results are shown for different modes of operation.

Contents

List of Figures	iii
1 LLC Resonant Converter	1
1.1 Resonant frequency in LLC resonant converter	1
1.1.1 Operation At, Below, and Above f_r	2
1.2 Modeling an LLC Half-Bridge converter	4
1.2.1 First Harmonic Approximation	4
1.2.2 Parameters estimation in FHA circuit model	5
1.2.3 Voltage-Gain Function	6
1.2.4 Calculation of normalized frequency at maximum gain	8
1.3 Observation from Voltage-Gain characteristics	9
1.4 ZVS and ZCS in LLC Resonant converter	11
2 Design Considerations for LLC resonant converter	15
2.1 Basic Requirements in designing	15
2.1.1 Line Regulation:	15
2.1.2 Load Regulation	17
2.1.3 Efficiency	17
2.2 Design Parameter and Simulation results	17
2.2.1 Design Steps	17
3 Conclusion and Future Work	23
3.1 Conclusion	23
3.2 Future Work	23

List of Figures

1.1	LLC resonant half-bridge converter	1
1.2	Operation at f_r	2
1.3	Operation below f_r	3
1.4	Operation above f_r	4
1.5	Model of LLC resonant half-bridge converter	5
1.6	Normalized frequency at maximum gain for $L_n = 5, Q_e = 1$	8
1.7	Gain vs Normalized frequency for different values of L_n and Q_e	10
1.8	M_g vs L_n for fixed Q_e	11
1.9	Input Impedance	11
1.10	Input Impedance	14
1.11	Boundary between ZVS and ZCS	14
2.1	Resonant current waveform at f_r , less than f_r , and more than f_r	15
2.2	Operation boundary for a case of $M_{g,max}$ and $M_{g,min}$	16
2.3	Maximum and minimum gain curve	18
2.4	M_g vs f_n for $f_{n,min}$ calculation	19

Chapter 1

LLC Resonant Converter

The LLC converter configuration has three main parts: Power switches, resonant circuit, rectifier for DC Output

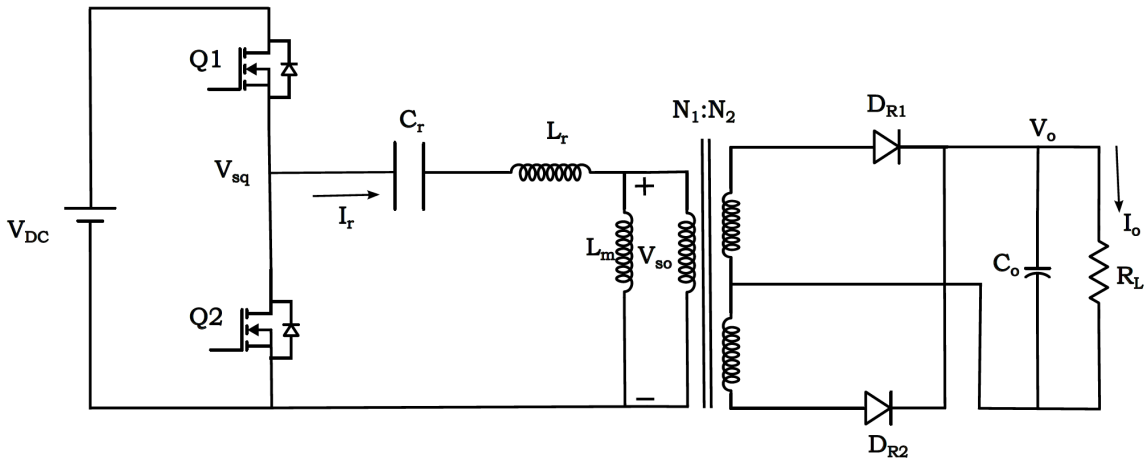


Figure 1.1: LLC resonant half-bridge converter

The switches Q1 and Q2 are set up to generate a square wave, which produces a unipolar square wave voltage. This is achieved by operating the power switches with 50 percent duty cycles that alternate for each switch. It's crucial to incorporate a small time gap between successive switch transitions. This will eliminate the risk of cross-conduction and help achieve ZVS.

The resonant network comprises capacitance (C_r), inductance (L_r) in series, and the magnetizing inductance (L_m) of the transformer. The transformer turns ratio is N_1/N_2 . The transformer offers electrical isolation and a turns ratio to supply the necessary output voltage.

The secondary part of the converter is comprised of a full-wave rectifier, which transforms the AC input into a DC output, providing power to the load R_L . The rectified voltage and current are smoothed by the output capacitor. The rectifier network can be implemented as a full-wave bridge or center-tapped configuration, with a capacitive filter as shown in fig (1.1).

1.1 Resonant frequency in LLC resonant converter

In the LLC resonant converter the frequency at peak resonance is a function of load due to addition of magnetizing inductance of transformer. The frequency at peak resonance (f_{co}) is varied within the range of f_{nl} to f_r as the variation in load.

At no load,

$$f_{co} = f_{nl} = \frac{1}{2\pi\sqrt{(L_r + L_m)C_r}} \quad (1.1)$$

At short circuit,

$$f_{co} = f_r = \frac{1}{2\pi\sqrt{L_r C_r}} \quad (1.2)$$

1.1.1 Operation At, Below, and Above f_r

From fig (1.1), the primary current is the sum of the magnetizing current and the secondary-side current referred to the primary. However, the magnetizing current flows only on the primary side and does not contribute to the power transferred from the primary side to secondary side.

Operation At Resonance:

- The resonant current decreases to the value of the magnetizing current fig (1.2) When switch Q1 turns off and no additional power is transferred to the secondary side.
- By introducing a delay in the activation time of switch Q2, the circuit achieves Zero Voltage Switching (ZVS) on the primary side and achieves a soft commutation of the rectifier diodes on the secondary side.

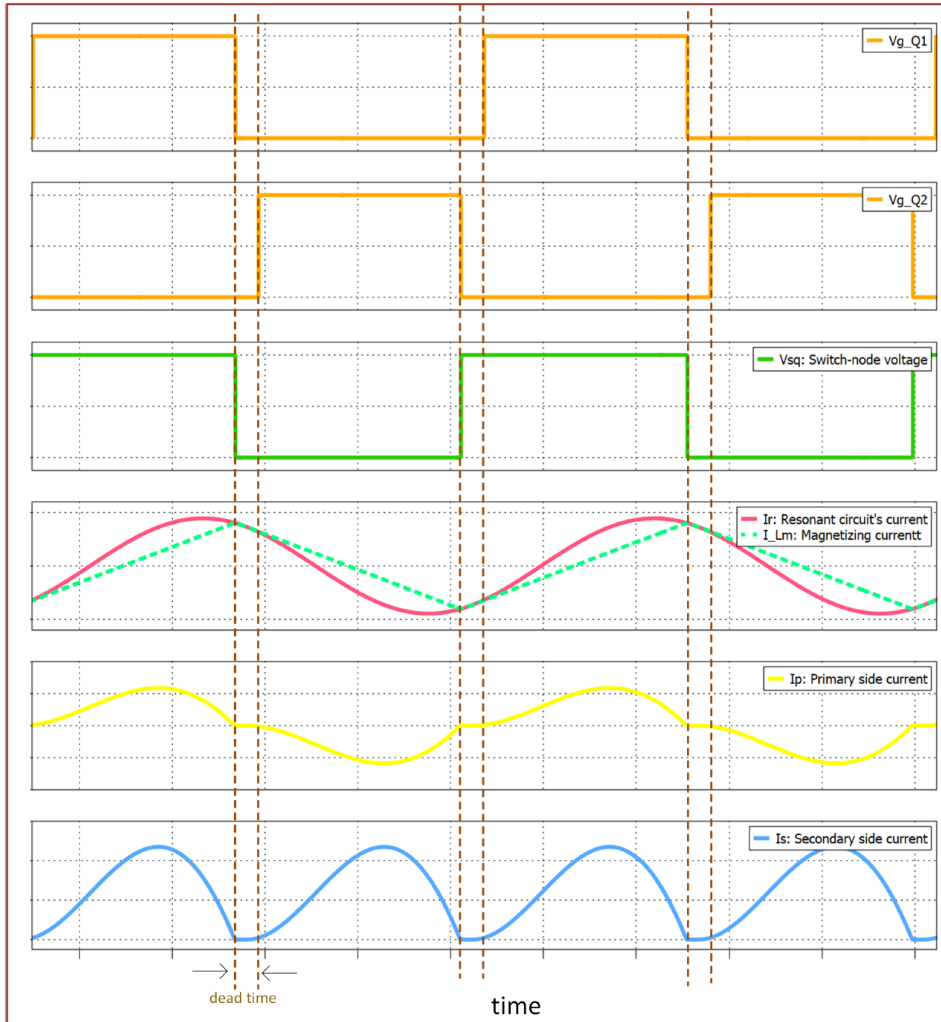


Figure 1.2: Operation at f_r

Operation Below Resonance:

- The resonant current falls to the same value as the magnetizing current before the end of the gate pulse width. Due to this, no power transfer occurs, even though the magnetizing current continues.
- The diodes on the secondary side operate in discontinuous current mode. So for the same amount of energy transfer to the load, more circulating current will flow in the resonant circuit which results in higher conduction losses on both the primary and secondary sides.
- The ZVS condition is still applicable at less than resonance frequency but not if the frequency becomes too low then the primary ZVS condition will not occur. We will see more on it in section.

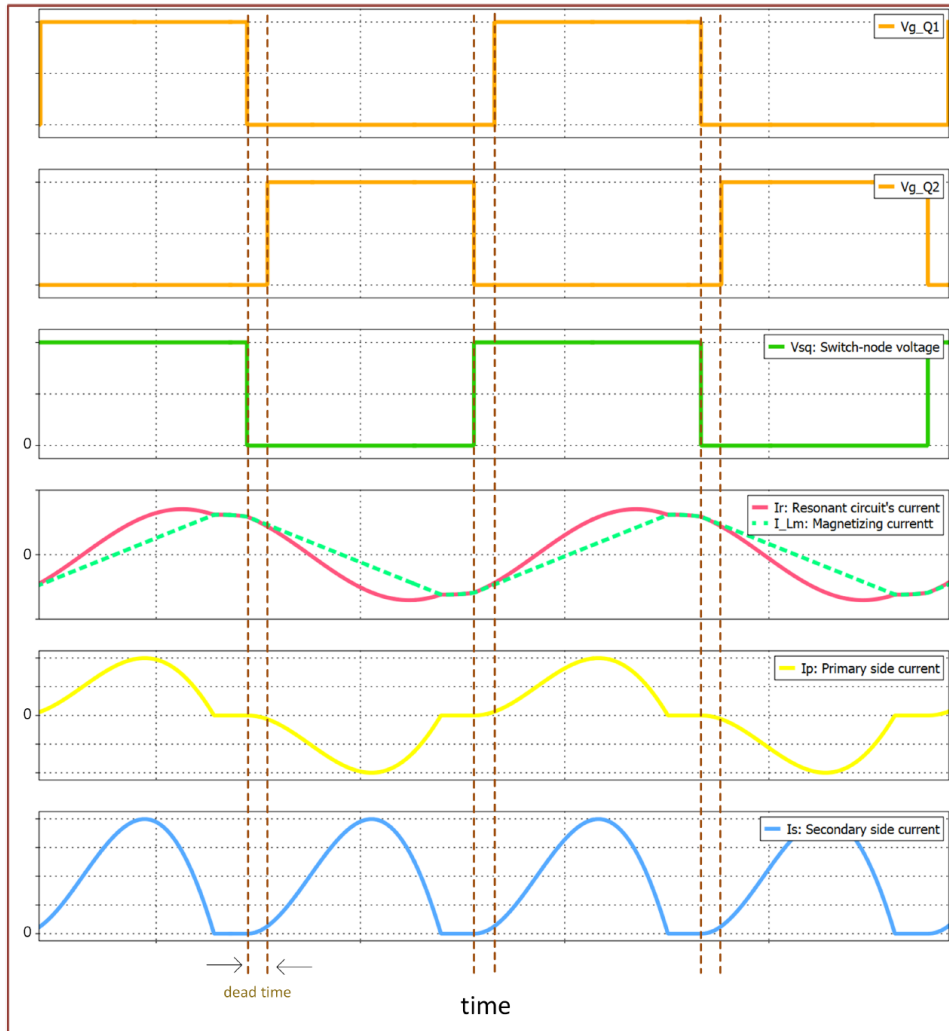


Figure 1.3: Operation below f_r

Operation Above Resonance:

- At the primary side of the resonant circuit, the circulating current is smaller. This leads to a decrease in conduction loss as the current within the resonant circuit operates continuously, which reduces the RMS value of current for the equivalent load.
- The rectifier diodes are not softly commutated and reverse recovery losses exist. However, when operated above f_r , it consistently attains primary Zero Voltage Switching.

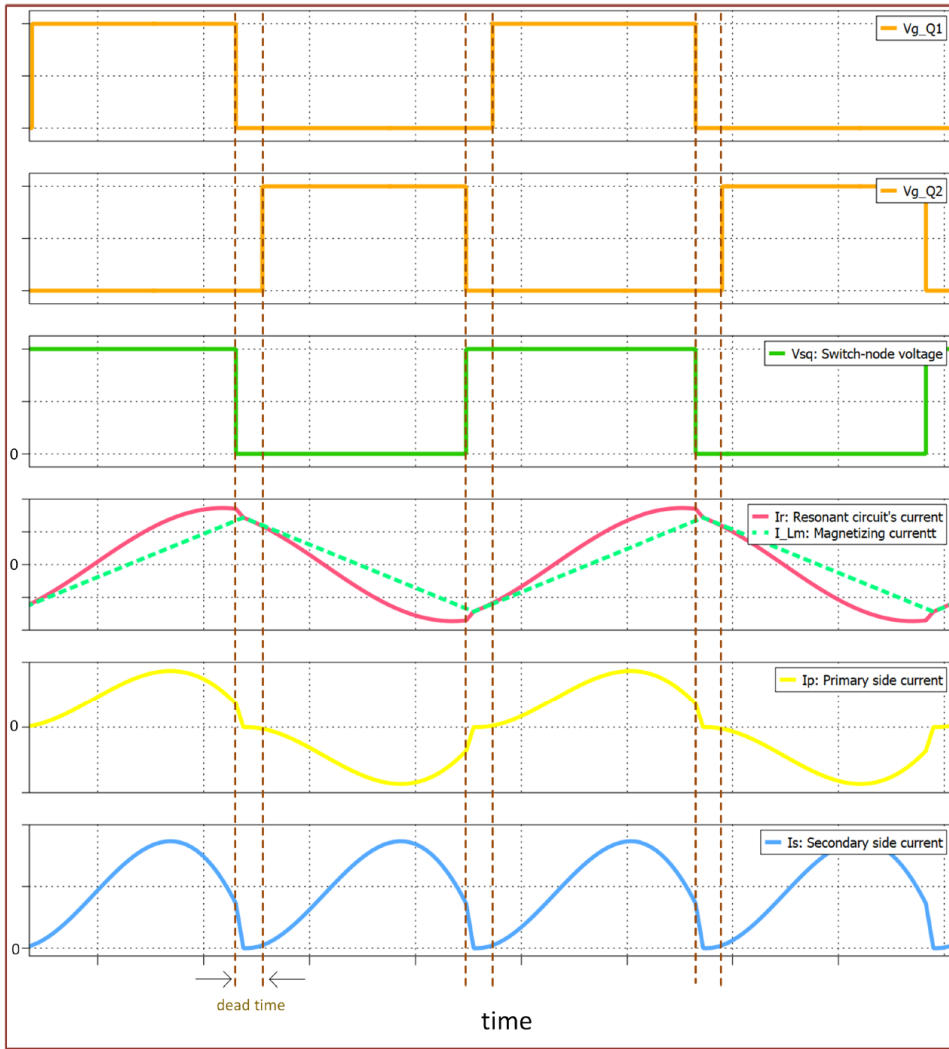


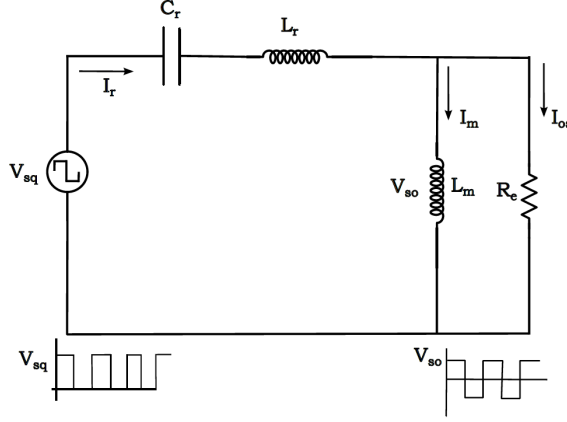
Figure 1.4: Operation above f_r

1.2 Modeling an LLC Half-Bridge converter

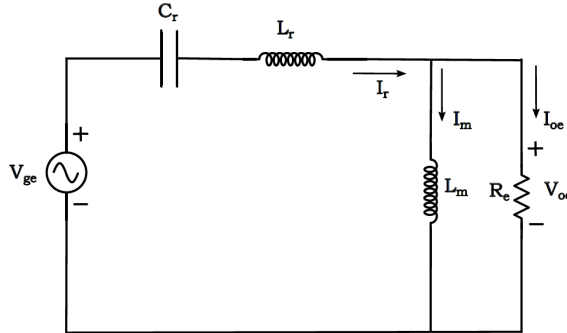
1.2.1 First Harmonic Approximation

This technique finds application in the modeling of an LLC Half-Bridge converter, if it operates at or near series resonance. This method is used to derive the gain function. We can represent the unipolar square wave voltage output (V_{sq}) of half bridge inverter and the current of the resonant tank with their fundamental components by ignoring all the higher-order harmonics.

An equivalent circuit of the LLC resonant half-bridge converter is represented in fig1.5 by ignoring the effect from the output capacitor and the transformer's secondary side leakage inductance. Also in this schematic, the secondary side variables are referred to the primary side and represented with only their fundamental components using first harmonic approximation (FHA). The circuit model using the first harmonic approximation is as shown in fig (1.5).



(a) Equivalent circuit without FHA



(b) Equivalent circuit with FHA

Figure 1.5: Model of LLC resonant half-bridge converter

1.2.2 Parameters estimation in FHA circuit model

The fundamental voltage of V_{sq} at the input side of the resonant tank,

$$v_{ge}(t) = \frac{2V_{DC}}{\pi} \sin 2\pi f_s t \quad (1.3)$$

$$V_{ge} = \frac{\sqrt{2}V_{DC}}{\pi} \quad (1.4)$$

The fundamental voltage at the input side,

$$v_{oe}(t) = \frac{4V_o}{\pi} * \frac{N_1}{N_2} \sin(2\pi f_s t - \phi_v) \quad (1.5)$$

where ϕ_v is the difference in phase between v_{oe} and v_{ge}

$$V_{oe} = \frac{2\sqrt{2}V_o}{\pi} * \frac{N_1}{N_2} \quad (1.6)$$

The average output current can be expressed as,

$$I_o = \frac{2I_{oe,m}}{\pi} \quad (1.7)$$

where $I_{oe,m}$ is the peak input current to the full wave rectifier

The fundamental component of current corresponding to V_{oe} and I_{oe} is,

$$i_{oe}(t) = I_{oe,m} * \frac{N_2}{N_1} * \sin(2\pi f_s t - \phi_i) = \frac{\pi}{2} * I_o * \frac{N_2}{N_1} * \sin(2\pi f_s t - \phi_i) \quad (1.8)$$

The RMS value of i_{oe} is,

$$I_{oe} = \frac{\pi}{2\sqrt{2}} * \frac{N_2}{N_1} * I_o \quad (1.9)$$

The AC equivalent load resistance R_e is,

$$R_e = \frac{V_{oe}}{I_{oe}} = \frac{\frac{2\sqrt{2}V_o}{\pi} * \frac{N_1}{N_2}}{\frac{\pi}{2\sqrt{2}} * \frac{N_2}{N_1} * I_o} = \frac{8}{\pi^2} * \left(\frac{N_1}{N_2}\right)^2 * R_L \quad (1.10)$$

$$R_e = \frac{8}{\pi^2} * \left(\frac{N_1}{N_2}\right)^2 * R_L$$

The FHA equivalent circuit is a single-frequency sinusoidal AC circuit, so we can calculate the reactances of C_r , L_r , and L_m as follows,

$$\omega_s = 2\pi f_s \quad (1.11)$$

$$X_{Cr} = \frac{1}{\omega_s C_r}, X_{Lr} = \omega_s L_r, X_{Lm} = \omega_s L_m \quad (1.12)$$

The RMS value of magnetizing current,

$$I_m = \frac{V_{oe}}{\omega_s L_m} = \frac{2\sqrt{2}}{\pi} * \frac{N_1}{N_2} * \frac{V_o}{\omega_s L_m} \quad (1.13)$$

The current flowing in the series resonant circuit is,

$$I_r = \sqrt{I_m^2 + I_{oe}^2} \quad (1.14)$$

1.2.3 Voltage-Gain Function

The input voltage and output voltage can be related in terms of their ratio or gain:

$$M_{g,DC} = \frac{N_1}{N_2} * \frac{V_o}{\frac{V_{dc}}{2}} \quad (1.15)$$

The ratio of AC voltage, $M_{g,AC}$ can be calculated by using the FHA,

$$M_{g,AC} = \frac{V_{so}}{V_{sq}} = \frac{V_{oe}}{V_{ge}} \quad (1.16)$$

from equation (1.15), (1.4) and (1.6)

$$M_{g,DC} = \frac{N_1}{N_2} * \frac{\frac{N_1}{N_2} * \frac{\pi}{2\sqrt{2}} V_{oe}}{\frac{V_{ge}}{2\sqrt{2}}} = \frac{V_{oe}}{V_{ge}}$$

$$M_{g,DC} = M_{g,AC} = \frac{V_{oe}}{V_{ge}} \quad (1.17)$$

Now from Fig.1.5, by applying voltage division,

$$\frac{V_{oe}}{V_{ge}} = \frac{jX_{Lm} \| R_e}{(jX_{Lm} \| R_e) + j(X_{Lr} - X_{Cr})} = \frac{(j\omega_s L_m) \| R_e}{(j\omega_s L_m) \| R_e + j\omega_s L_r + \frac{1}{j\omega_s C_r}}$$

Hence the gain magnitude is

$$M_g = \left| \frac{(j\omega_s L_m) \| R_e}{(j\omega_s L_m) \| R_e + j\omega_s L_r + \frac{1}{j\omega_s C_r}} \right| \quad (1.18)$$

Switching to s -domain ($s = j\omega_s$) and simplifying the parallel term,

$$(sL_m) \| R_e = \frac{R_e sL_m}{R_e + sL_m},$$

we can write

$$M_g = \left| \frac{\frac{R_e sL_m}{R_e + sL_m}}{\frac{R_e sL_m}{R_e + sL_m} + sL_r + \frac{1}{sC_r}} \right| = \left| \frac{sL_m R_e \cdot sC_r}{s^3 L_r L_m C_r + s^2 [L_r + L_m] R_e C_r + sL_m + R_e} \right|.$$

Substituting $s = j\omega_s$ and rearranging gives an expression in terms of ω_s ,

$$M_g = \left| \frac{-L_m C_r \omega_s^2}{1 - L_r C_r (1 + \frac{L_m}{L_r}) \omega_s^2 + j \left[\frac{L_m \omega_s}{R_e} - \frac{L_r L_m C_r \omega_s^3}{R_e} \right]} \right|$$

Now, define the normalized quantities,

$$L_n = \frac{L_m}{L_r} \quad (1.19)$$

$$f_n = \frac{f_s}{f_r} \quad \text{with} \quad \omega_s = 2\pi f_s, \quad \omega_r = 2\pi f_r \quad (1.20)$$

$$Q_e = \frac{\sqrt{L_r/C_r}}{R_e} \quad (1.21)$$

With these substitutions the voltage gain can be compactly expressed as

$$M_g = \left| \frac{L_n f_n^2}{[(L_n + 1)f_n^2 - 1] + j[(f_n^2 - 1) f_n Q_e L_n]} \right| \quad (1.22)$$

$$M_g = \frac{L_n f_n^2}{\sqrt{[(L_n + 1)f_n^2 - 1]^2 + [(f_n^2 - 1) f_n Q_e L_n]^2}} \quad (1.23)$$

The relationship between input and output voltages are,

$$V_o = M_g(f_n, L_n, Q_e) \frac{N_2}{N_1} \frac{V_{DC}}{2} \quad (1.24)$$

1.2.4 Calculation of normalized frequency at maximum gain

To calculate the normalized frequency at maximum gain, we have to differentiate Equation (1.23) with respect to f_n :

$$\frac{dM_g}{df_n} = 0$$

After differentiation of Equation(1.23) and simplification, we obtain

$$\begin{aligned} 2 - 2(L_n + 1)f_n^2 - f_n^6 Q_e^2 L_n^2 + f_n^2 Q_e^2 L_n^2 &= 0 \\ 2[1 - (L_n + 1)f_n^2] + f_n^2 Q_e^2 L_n^2 [1 - f_n^4] &= 0 \end{aligned} \quad (1.25)$$

By using the above Equation 1.25, we can calculate the frequency at which the maximum gain will occur for a fixed value of L_n and Q_e .

For example, for $L_n = 5$ and $Q_e = 1$, the maximum gain occurs by solving

$$2 + 13f_n^2 - 25f_n^6 = 0$$

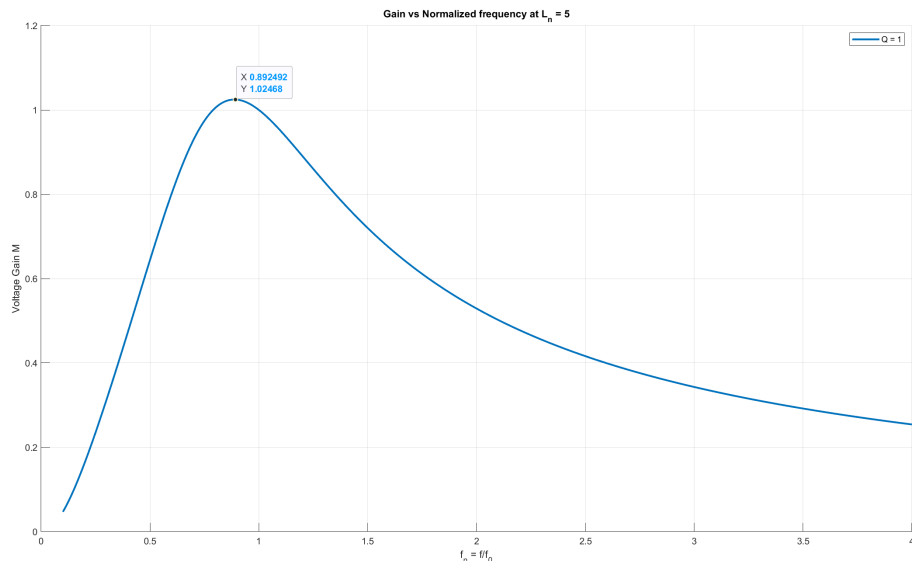
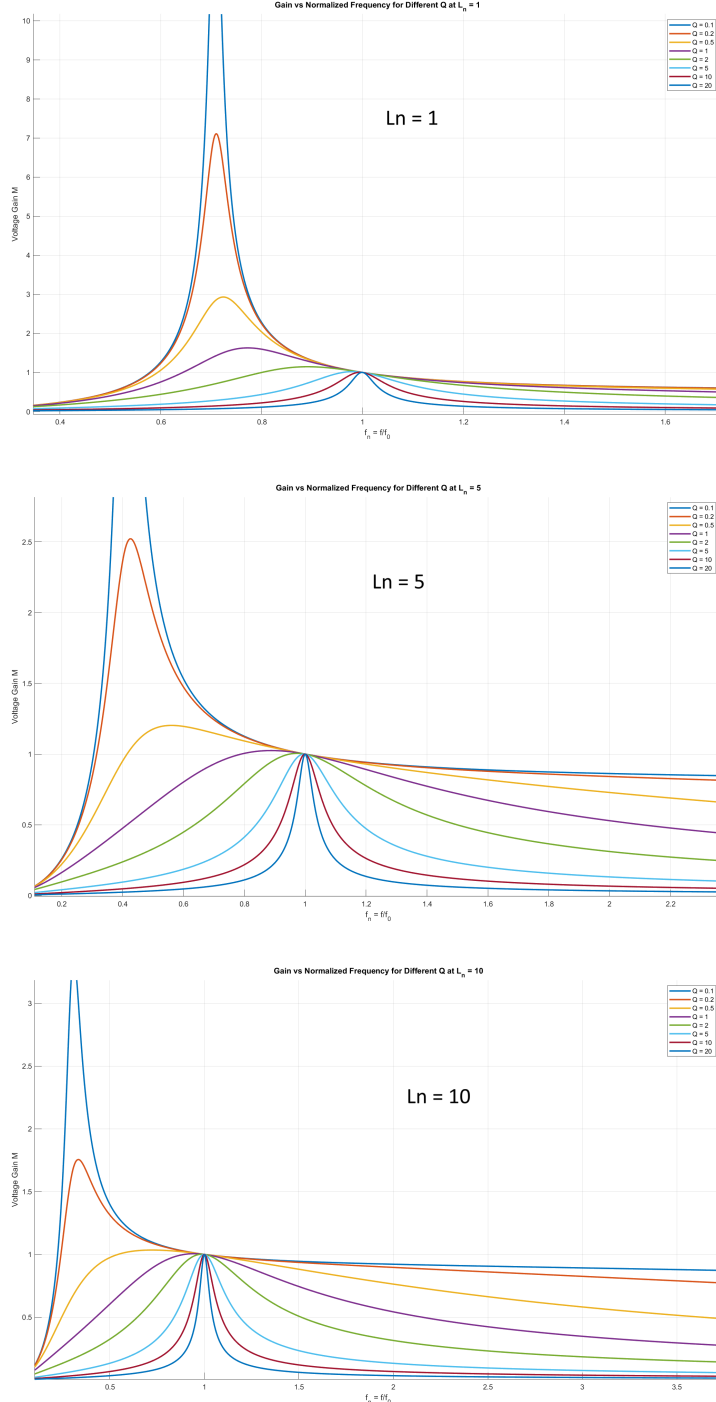


Figure 1.6: Normalized frequency at maximum gain for $L_n = 5, Q_e = 1$

1.3 Observation from Voltage-Gain characteristics

From Equation (1.23), we can see that gain depends on normalized frequency (f_n), normalized inductance (L_n), and quality factor (Q_e). In the gain function, normalized frequency (f_n) is the control variable. L_n and Q_e are fixed once the design is finalized.

The gain is adjusted by f_n after completing the design. Figure (1.7) shows how gain varies with normalized frequency for different values of Q_e at a fixed L_n . Each plot corresponds to a fixed L_n and shows a family of curves for Q_e ranging from 0.1 to 10.



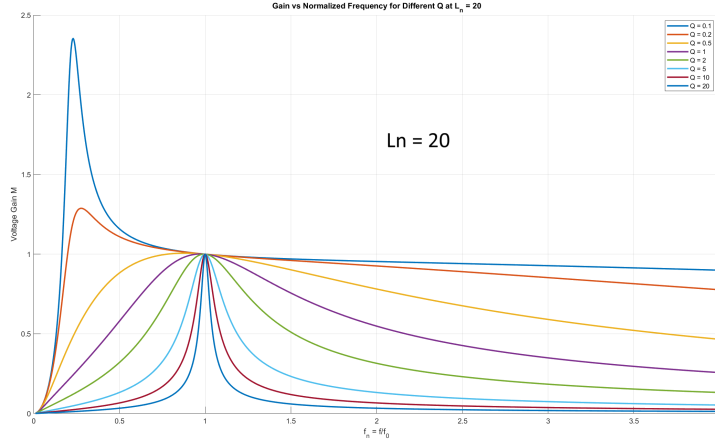


Figure 1.7: Gain vs Normalized frequency for different values of L_n and Q_e

Observations:

1. For a given value of L_n and Q_e , M_g exhibits convex behavior near the circuit's resonant frequency. The frequency f_n corresponding to the peak value shifts with load variation (and thus with Q_e) for a given L_n , since Q_e is load-dependent as described in Eq.(1.21).
2. All curves converge at the point $(f_n, M_g) = (1, 1)$ regardless of the L_n and Q_e combination. At this point $f_n = 1$ (i.e., $f_s = f_r$); at f_r , the impedance of $L_r - C_r$ is zero ($X_{L_r} - X_{C_r} = 0$). Thus, the input voltage directly appears at the output, giving unity gain ($M_g = 1$). This also follows from Eq.(1.23) by substituting $f_n = 1$.
3. The point $(f_n, M_g) = (1, 1)$ is independent of load. If the switching frequency equals the series-resonance frequency, the gain will always be unity regardless of load current.
4. For a fixed L_n , increasing Q_e compresses the curve, producing a narrower frequency-control band. As Q_e increases, the peak gain decreases and the normalized frequency corresponding to the peak value of M_g moves closer to $f_n = 1$.
5. From Eq.(1.21), reducing R_L increases Q_e . This holds true when L_m , L_r , and C_r remain constant. Since R_L is in parallel with L_m , reducing R_L diminishes the effect of L_m and shifts the peak-resonance frequency (f_{co}) toward the series-resonance frequency (f_r).

(a) At no-load ($R_L \rightarrow \infty$, $Q_e = 0$), from the equivalent circuit:

$$f_{co} = \frac{1}{2\pi\sqrt{(L_r + L_m)C_r}} = f_{nl}, \quad f_r = \frac{1}{2\pi\sqrt{L_r C_r}},$$

so

$$\frac{f_{nl}}{f_r} = \sqrt{\frac{L_r}{L_r + L_m}} = \frac{1}{\sqrt{1 + L_n}}.$$

At $f_s = f_{nl}$,

$$M_g|_{f_s=f_{nl}} = \frac{L_m + L_r}{L_m} \cdot \frac{R_e}{\sqrt{\frac{L_r}{C_r}}} \quad (1.26)$$

or equivalently

$$M_g|_{f_s=f_{nl}} = \frac{1 + L_n}{L_n} \cdot \frac{1}{Q_e}. \quad (1.27)$$

- (b) If the load is shorted ($R_L = 0$, $Q_e \rightarrow \infty$), then L_m is bypassed. In this condition the effect of L_m on gain vanishes.

6. If R_L changes from infinity to zero, the resonant-peak gain decreases from infinity to unity, and the corresponding f_{co} moves from f_{nl} to f_r .
7. Reducing L_n (for fixed Q_e) compresses the curve and moves f_{co} toward f_r , as shown in Fig.(1.3), thereby improving frequency-control range and increasing peak gain. This occurs because:
 - (i) A decrease in L_n (via smaller L_m) moves f_{nl} closer to f_r and the curve squeezes from f_{nl} to f_r .
 - (ii) A decrease in L_n is due to an increase in L_r which raises Q_e . This, further shrinks the curve.

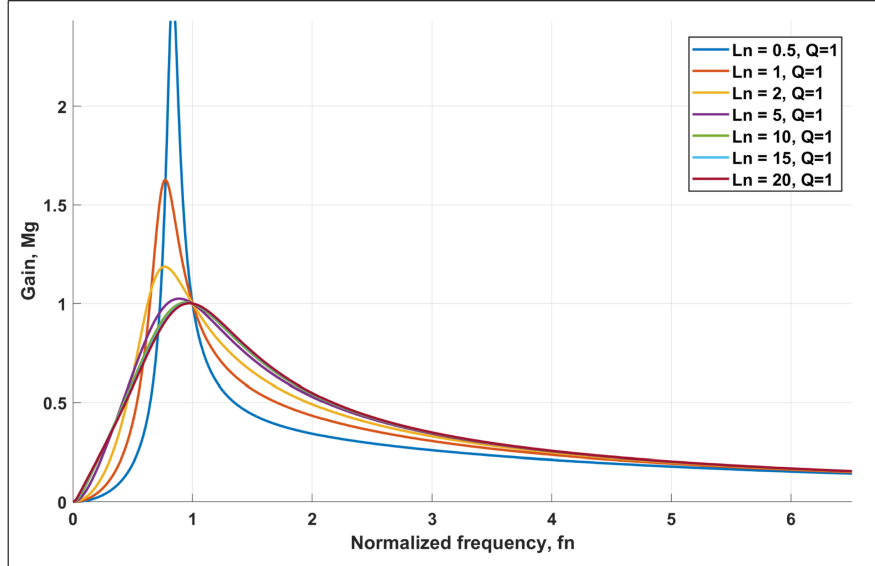


Figure 1.8: M_g vs L_n for fixed Q_e

1.4 ZVS and ZCS in LLC Resonant converter

To understand Zero Voltage Switching (ZVS) and Zero Current Switching (ZCS), we first analyze how the input impedance changes with respect to the switching frequency.

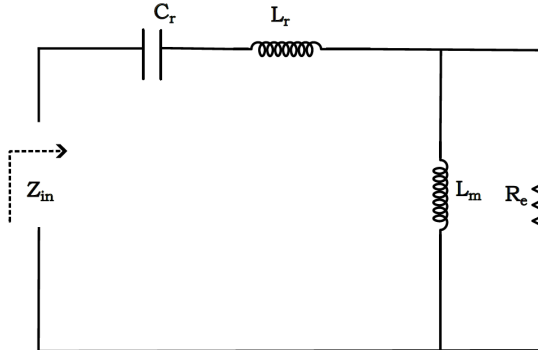


Figure 1.9: Input Impedance

$$Z_{in} = j\omega_s L_r + \frac{1}{j\omega_s C_r} + (R_e \parallel j\omega_s L_m) \quad (1.28)$$

Simplifying,

$$Z_{in} = j\omega_s L_r + \frac{1}{j\omega_s C_r} + \frac{R_e j\omega_s L_m}{R_e + j\omega_s L_m}$$

Expanding the above expression gives:

$$Z_{in} = \frac{R_e(\omega_s L_m)^2}{R_e^2 + (\omega_s L_m)^2} + j \left(\omega_s L_r - \frac{1}{\omega_s C_r} + \frac{R_e^2 \omega_s L_m}{R_e^2 + (\omega_s L_m)^2} \right) \quad (1.29)$$

Case 1: $f_s > f_r$

When the switching frequency is greater than the series resonant frequency:

$$\omega_s > \omega_r = \frac{1}{\sqrt{L_r C_r}} \Rightarrow \omega_s L_r > \frac{1}{\omega_s C_r}$$

From Eq.(1.29), the input impedance is always inductive for this case.

Case 2: $f_s = f_r$

At the series resonance frequency:

$$\omega_s = \omega_r = \frac{1}{\sqrt{L_r C_r}} \Rightarrow \omega_s L_r = \frac{1}{\omega_s C_r}$$

Hence,

$$Z_{in} = \frac{R_e(\omega_s L_m)^2}{R_e^2 + (\omega_s L_m)^2} + j \frac{R_e^2 \omega_s L_m}{R_e^2 + (\omega_s L_m)^2}$$

The input impedance is always inductive in nature at this condition.

Case 3: $f_{nl} < f_s < f_r$

$$\frac{1}{\sqrt{(L_r + L_m)C_r}} < \omega_s < \frac{1}{\sqrt{L_r C_r}}$$

In this range, the input impedance can be inductive or capacitive depending on R_e . At the boundary between the two regions, the imaginary part of Z_{in} is zero from Eq.(1.29)

$$\omega_s L_r - \frac{1}{\omega_s C_r} + \frac{R_e^2 \omega_s L_m}{R_e^2 + (\omega_s L_m)^2} = 0$$

Rearranging,

$$\frac{1}{\omega_s C_r} - \omega_s L_r = \frac{R_e^2 \omega_s L_m}{R_e^2 + (\omega_s L_m)^2}$$

Solving for R_e :

$$R_e = \sqrt{\frac{\omega_s^2 L_m^2 - L_r C_r L_m^2 \omega_s^4}{L_m C_r \omega_s^2 + L_r C_r \omega_s^2 - 1}} \quad (1.30)$$

The critical resistance separating inductive and capacitive behavior is, therefore,

$$R_{\text{critical}} = \sqrt{\frac{\omega_s^2 L_m^2 - L_r C_r L_m^2 \omega_s^4}{L_m C_r \omega_s^2 + L_r C_r \omega_s^2 - 1}}$$

(1.31)

If $R_e > R_{critical}$, the input impedance is Inductive.

If $R_e < R_{critical}$, the input impedance is Capacitive.

Now, using the normalized quantities:

$$L_n = \frac{L_m}{L_r}, \quad Q_e = \frac{\omega_r L_r}{R_e}, \quad f_n = \frac{f_s}{f_r} = \frac{\omega_s}{\omega_r}$$

and substituting into Eq.(1.30), we can find frequency at the ZVS and ZCS boundary condition.

$$\frac{\omega_r L_r}{Q_e} = \sqrt{\frac{\omega_s^2 L_r^2 L_n^2 - \omega_s^4 L_r^3 L_n^2 C_r}{L_n L_r C_r \omega_s^2 + L_r C_r \omega_s^2 - 1}}$$

Simplifying and replacing $L_r C_r = 1/\omega_r^2$:

$$\frac{1}{Q_e^2} = \frac{L_n^2 \omega_s^2 / \omega_r^2 - L_n \omega_s^4 / \omega_r^4}{L_n \omega_s^2 / \omega_r^2 + \omega_s^2 / \omega_r^2 - 1}$$

In terms of normalized frequency $f_n = \omega_s / \omega_r$:

$$\frac{1}{Q_e^2} = \frac{L_n^2 f_n^2 - L_n f_n^4}{L_n f_n^2 + f_n^2 - 1} \quad (1.32)$$

After rearranging,

$$f_n^4 Q_e^2 L_n + f_n^2 [1 + L_n - L_n^2 Q_e^2] - 1 = 0 \quad (1.33)$$

The normalized frequency at the ZVS/ZCS boundary can be obtained as follows:

$$f_n = \sqrt{\frac{L_n^2 Q_e^2 - L_n - 1 + \sqrt{(1 + L_n - L_n^2 Q_e^2)^2 + 4 Q_e^2 L_n}}{2 Q_e^2 L_n}} \quad (1.34)$$

Case 4: $f_s < f_{nl}$

$$\omega_s < \omega_{nl} \omega_s < \frac{1}{\sqrt{(L_r + L_m) C_r}} \Rightarrow \omega_s (L_r + L_m) < \frac{1}{\omega_s C_r}$$

Hence, from Eq.(1.29), the input impedance is always Capacitive in this range. (for switching frequency less than the peak resonant frequency at no load)

Since the impedance is inductive in Cases 1 and 2, and also when $R_e > R_{critical}$ in Case 3, it means that the current I_r lags the applied voltage V_{ge} , satisfying the condition required for ZVS operation.

Fig.(1.10) shows the equivalent circuit of the resonant tank used to analyze Z_{in} and its phase.

$$Z_{in} = |Z_{in}| e^{j\phi_z} \quad (1.35)$$

where ϕ_z is the phase angle between V_{ge} and I_r . From Eq.(1.29), we can find the magnitude and phase of ϕ_z . ϕ_z varies from $-\pi/2$ to $+\pi/2$.

$\phi_z < 0 \Rightarrow Z_{in}$ is capacitive (I_r leads applied voltage V_{ge})

$\phi_z > 0 \Rightarrow Z_{in}$ is inductive (I_r lags applied voltage V_{ge})

$\phi_z = 0 \Rightarrow Z_{in}$ is resistive (I_r in phase with applied voltage V_{ge})

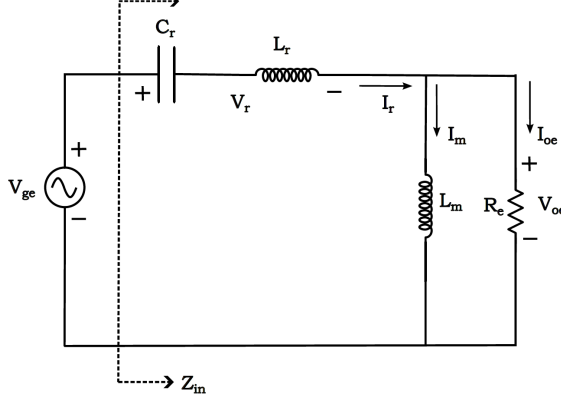


Figure 1.10: Input Impedance

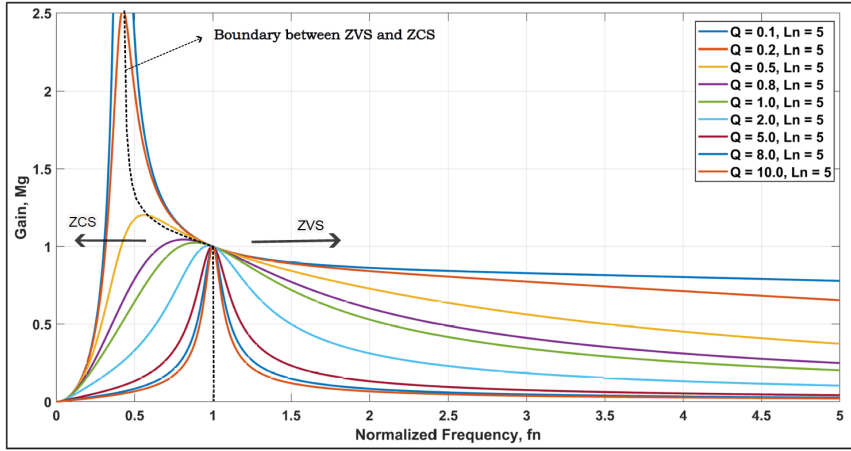


Figure 1.11: Boundary between ZVS and ZCS

Thus, ϕ_z acts as a boundary between the capacitive and inductive regions, as illustrated in Fig(1.11).

To achieve ZVS, the input phase angle should be positive ($\phi_z > 0$). From Fig.(1.11), all the peaks corresponding to frequency f_{co} lie in the capacitive region, but the boundary is very close to these peaks. To distinguish between resonant-peaks and the gain at the resonant boundary, we define the gain value at the boundary frequency as the attainable peak gain $M_{g,ap}$, which is usually close to the true maximum gain $M_{g,peak}$:

$$M_{g,peak} = M_g|_{f=f_{co}} \quad (1.36)$$

where f_{co} is the frequency at which the gain reaches its maximum value from Eq.(1.23). The maximum gain occurs as the switching frequency varies from zero to infinity for fixed L_m , L_r , C_r , and R_e .

Chapter 2

Design Considerations for LLC resonant converter

The output voltage of converter can be controlled by gain through controlling f_n

$$V_o = M_g(f_n, L_n, Q_e) * \frac{N_2}{N_1} * \frac{V_{DC}}{2}$$

The design needs to be function close to the series resonance or near fsw is equal to fr because the accuracy of the FHA is dependent on the circuit operating precisely at the resonance frequency fr, ensuring that only a pure sinusoidal current flows through the resonant circuit. We can see in Fig(2.1).

When designing a converter, the FHA approach can be used to create an initial design. However, it may be necessary to optimize and finalize the design through bench testing.

2.1 Basic Requirements in designing

The three basic requirements in the design of a power supply converter are: Line Regulation, load regulation, and efficiency.

2.1.1 Line Regulation:

Line regulation is the variation in output voltage due to variation in input voltage over a defined range, for a fixed load current. The line regulation can be achieved by using Eq(1.24).

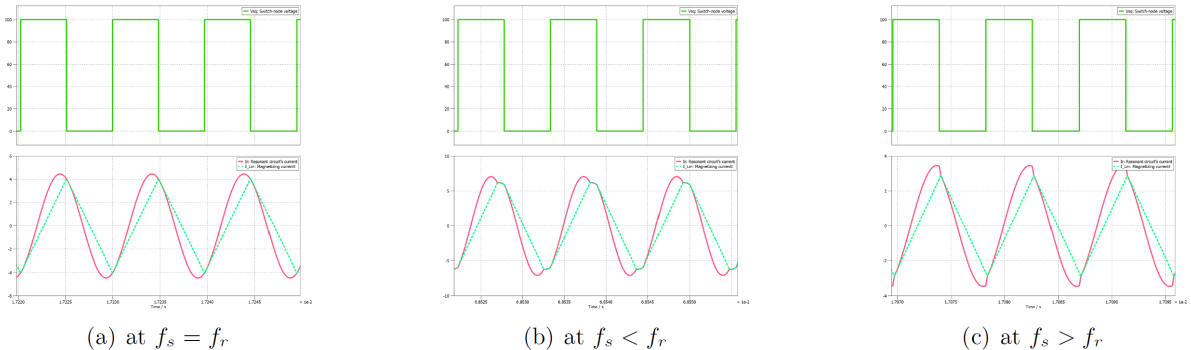


Figure 2.1: Resonant current waveform at f_s , less than f_r , and more than f_r

Let Assume $V_{o,min}$ and $V_{o,max}$ are the minimum and maximum output voltages respectively. If we choose transformer turns ratio as 1, then from Equation(1.24):

$$M_{g,max} = \frac{V_{o,max}}{\frac{V_{in,min}}{2}} \quad (2.1)$$

$$M_{g,min} = \frac{V_{o,min}}{\frac{V_{in,max}}{2}} \quad (2.2)$$

For $M_{g,max}$ and $M_{g,min}$ the switching frequency covers a range from minimum to maximum (f_{min} to f_{max}), in which the required gain should be achieved. From Fig.(2.2) we can see the frequency range for the chosen design. The frequency should be adjusted from minimum to maximum to achieve the line and load regulation requirements.

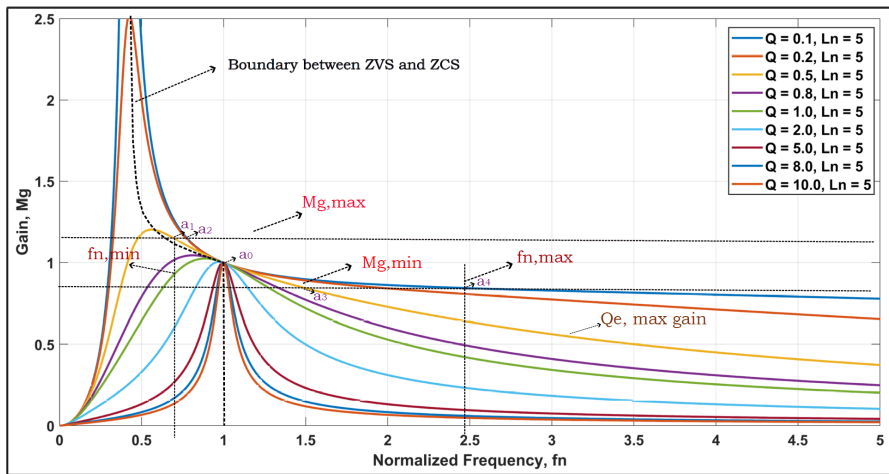


Figure 2.2: Operation boundary for a case of $M_{g,max}$ and $M_{g,min}$

We have to design the converter to meet the conditions mentioned in Equations (2.3) and (2.4). All possible values of gain must contain the gain in the range of minimum to maximum.

$$\text{For no-load } (I_o = 0) : (M_g > M_{g,no-load}) \supseteq (M_{g,min}, M_{g,max}) \quad (2.3)$$

$$\text{For } (I_o > 0) : (M_g \geq 0) \supseteq (M_{g,min}, M_{g,max}) \quad (2.4)$$

where $M_{g,no-load}$ is a value at $Q_e = 0$ and when $f_n \rightarrow \infty$, From Equation(1.23),

$$M_g = \frac{L_n f_n^2}{\sqrt{[(L_n + 1)f_n^2 - 1]^2 + [(f_n^2 - 1)f_n Q_e L_n]^2}}$$

$$M_g = \frac{L_n}{\sqrt{\left[(L_n + 1) - \frac{1}{f_n^2}\right]^2 + \left[\left(f_n - \frac{1}{f_n}\right) Q_e L_n\right]^2}}$$

If $f_n \rightarrow \infty$ and $Q_e \neq 0$

$$M_g = 0$$

If $f_n \rightarrow \infty$ and $Q_e = 0$

$$M_{g,no-load} = \frac{L_n}{L_n + 1} \quad (2.5)$$

When ($Q_e = 0$), the gain curve is governed solely by (L_n); therefore pick (L_n) to satisfy Eq.(2.3).

For ($Q_e \neq 0$), select an appropriate design curve (i.e., choose (L_n) and operating conditions) so that the resulting gain range meets Eq.(2.4).

2.1.2 Load Regulation

Normal Load operation: From Fig.(2.2), for a fixed L_n , the gain curve shifts lower and closer to f_r with a reduced peak as load increases. Therefore, as load current rises, the gain curve moves from its no-load configuration to a lower magnitude. $Q_{e,\text{max-gain}}$ denotes the curve corresponding to the maximum load current while satisfying Eq.(2.4).

If the load increases beyond $Q_{e,\text{max-gain}}$, then the new curve will not coincide with $M_{g,\text{max}}$ line, due to this output-voltage regulation is lost and design modification will be required.

2.1.3 Efficiency

Efficiency is one of the primary advantages of an LLC resonant converter. Primary-side ZVS can be achieved over a wide operating range, minimizing switching losses and improving converter efficiency.

2.2 Design Parameter and Simulation results

The design specifications for dc-dc LLC resonant converter are given in the table below:

Input dc voltage (V_{in})	390 - 410 V
Output voltage (V_{out})	36 - 57 V
V_{in} (nominal)	400 V
V_{out} (nominal)	48 V
Output power (P_{out})	1200 W
Resonance frequency (f_r)	100 kHz

Table 2.1: Design specification for LLC resonant dc-dc converter

2.2.1 Design Steps

1. Transformer Turns Ratio ($\frac{N_1}{N_2}$)

From Eq.(1.24),

$$\frac{N_1}{N_2} = M_g \times \frac{V_{in}}{2V_o}$$

For nominal input and output voltage:

$$\begin{aligned} \frac{N_1}{N_2} &= \left(\frac{\frac{V_{in,nominal}}{2}}{V_{o,nominal}} \right)_{M_g=1} \\ \frac{N_1}{N_2} &= \frac{400/2}{48} = 4.166 \\ \boxed{\frac{N_1}{N_2} \approx 5} \end{aligned} \tag{2.6}$$

Thus, the transformer turns ratio should be selected as 5.

2. Maximum and Minimum Gain for Converter

Using Eq.(2.1) and (2.2),

$$M_{g,max} = \left(\frac{V_{o,max}}{V_{in,min}/2} \right) \left(\frac{N_1}{N_2} \right)$$

$$M_{g,max} = 5 \times \frac{57}{390/2} = \boxed{1.4615} \quad (2.7)$$

$$M_{g,min} = \left(\frac{V_{o,min}}{V_{in,max}/2} \right) \left(\frac{N_1}{N_2} \right)$$

$$M_{g,min} = 5 \times \frac{36}{410/2} = \boxed{0.8781} \quad (2.8)$$

3. Selection of L_n and Q_e

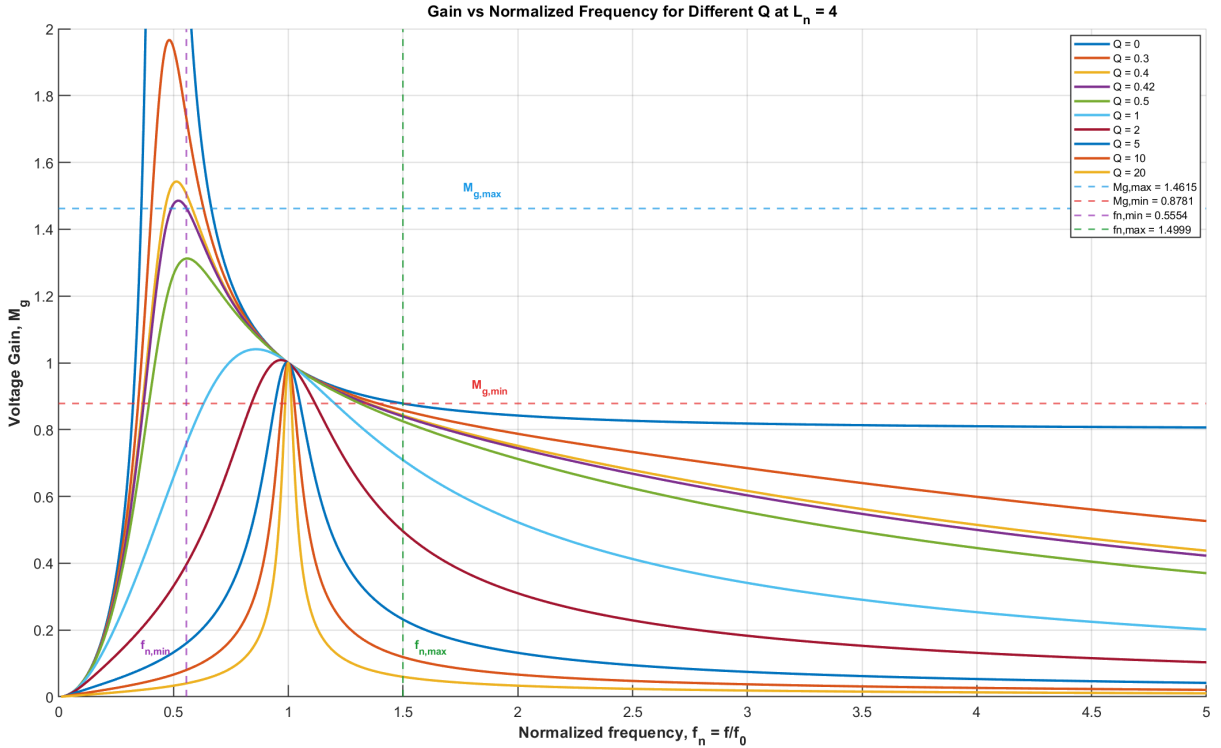


Figure 2.3: Maximum and minimum gain curve

From Equation (6.3), the minimum gain line should coincide with the $Q_e = 0$ curve, corresponding to a no-load condition. This implies that minimum gain occurs at no load. For varying load conditions, the maximum gain must be achieved. Referring to Fig.(2.3), if we select $L_n = 4$ and $Q_e = 0.42$, the required maximum gain can be achieved. For $Q_e > 0.42$, the condition of Eq.(2.4) is not satisfied.

We need a switching frequency range ($f_{n,min}$ to $f_{n,max}$) within which the converter can operate to achieve the required gain. For calculating $f_{n,max}$, we can do it in two ways: either by finding the point where the $M_{g,min}$ line coincides with the no-load curve ($Q_e = 0$) in the Fig.(2.3), or by setting $Q_e = 0$ in Eq.(1.23).

So, to calculate Normalized Frequency Range for $Q_e = 0$,

$$f_{n,max} = \sqrt{\frac{M_{g,min}}{M_{g,min}(L_n + 1) - L_n}} \quad (2.9)$$

Substituting $M_{g,min} = 0.8781$, $M_{g,max} = 1.4615$ and $L_n = 4$:

$$f_{n,max} = 1.4999 \quad (2.10)$$

When selecting $f_{n,min}$, it's important to consider the boundaries for ZVS and ZCS. Such that all resonant peaks fall within the capacitive region. The ZVS boundary line is very close to the peak gain, so we always allow for some margin when selecting the $Q_{e,max}$ from M_g vs f_n . For $Q_{e,max} = 0.42$, from Fig.(2.4) the achievable peak gain is 1.485, while the maximum gain for our converter is 1.461, which provides a sufficient margin from the boundary condition. With a $Q_{e,max}$ of 0.42 and $M_{g,max}$, we are in the ZVS region.

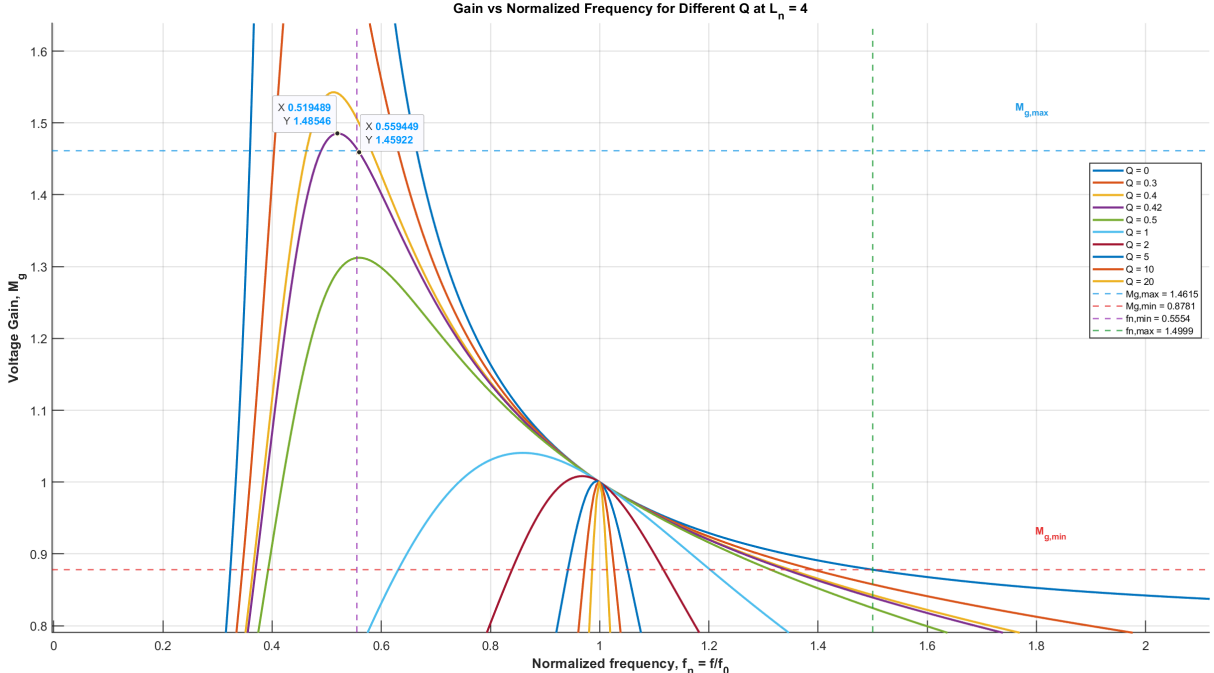


Figure 2.4: M_g vs f_n for $f_{n,min}$ calculation

From Fig.(2.4),

$$f_{n,min} = 0.5554 \quad (2.11)$$

Since $f_r = 100$ kHz,

$$f_{s,min} = 55.54 \text{ kHz, and } f_{s,max} = 149.99 \text{ kHz} \quad (2.12)$$

The operating frequency range is thus 55.54 kHz to 149.99 kHz.

4. Equivalent Load Resistance (R_e)

From Eq.(1.10),

$$R_e = \frac{8}{\pi^2} \left(\frac{N_1}{N_2} \right)^2 R_L$$

Substituting values:

$$R_e = \frac{8}{\pi^2} \times 25 \times \frac{48}{25}$$

$$R_e = 38.9468 \Omega \quad (2.13)$$

5. Calculation of Resonant Circuit Parameters

Using the definition of quality factor:

$$Q_e = \frac{\sqrt{\frac{L_r}{C_r}}}{R_e} = \frac{1}{\omega_r R_e C_r}$$

Hence,

$$C_r = \frac{1}{\omega_r R_e Q_e} = \frac{1}{2\pi \times 100 \times 10^3 \times 38.9468 \times 0.42}$$

$$C_r = 97.3463 \text{ nF} \quad (2.14)$$

The resonant inductance:

$$L_r = \frac{1}{(2\pi f_r)^2 C_r} = 26.05 \mu\text{H} \quad (2.15)$$

Magnetizing inductance:

$$L_m = L_n L_r = 4 \times 26.05 \mu\text{H} = 104.2 \mu\text{H} \quad (2.16)$$

6. Calculation of Primary and Secondary Currents

From Eq.(1.9)

$$I_{p1} = \frac{\pi}{2\sqrt{2}} * \frac{N_2}{N_1} * I_o = \frac{\pi}{2\sqrt{2}} * \frac{1}{5} * 25$$

$$I_{p1} = 5.55 \text{ A} \quad (2.17)$$

RMS magnetizing current at $f_{s,min}$ (maximum value) from Eq.(1.13)

$$I_m = \frac{2\sqrt{2}}{\pi} \frac{N_1}{N_2} \frac{V_o}{\omega_s L_m}$$

$$I_m = 5.899 \text{ A}$$

The rated resonant current,

$$I_r = \sqrt{I_m^2 + I_{p1}^2} = 8.1 \text{ A}$$

Secondary winding current,

$$I_{s1} = \frac{N_1}{N_2} I_{p1} = 27.75 \text{ A}$$

Transformer rated current in each winding,

$$I_{s,rated} = \frac{\sqrt{2} I_{s1}}{2} = \frac{\sqrt{2} * 27.75}{2} = 19.626 \text{ A}$$

7. Selection of Resonant Inductor

Resonant inductance $L_r = 26.05 \mu\text{H}$, Rated resonant current $I_{Lr,\text{rated}} = 8.1 \text{ A}$

AC voltage across L_r at $f_{s,\min}$ and $f_{s,\max}$:

$$V_{Lr}(f_{s,\min}) = \omega_{s,\min} L_r I_{Lr,\text{rated}} = 2\pi \cdot 55.55 \times 10^3 \cdot 26.05 \times 10^{-6} \cdot 8.1 = 74.206 \text{ V}$$

$$V_{Lr}(f_{s,\max}) = \omega_{s,\max} L_r I_{Lr} = 2\pi \cdot 149.99 \times 10^3 \cdot 26.05 \times 10^{-6} \cdot 5.9 = 144.955 \text{ V}$$

Frequency range: 55.55 kHz to 14.99 kHz

8. Selection of Resonant Capacitor

Using $Q_e = \frac{1}{\omega_r R_e C_r}$, the resonant capacitor is:

$$C_r = 97.3463 \text{ nF.}$$

Resonant-capacitor AC voltage (at rated resonant current $I_r = 8.1 \text{ A}$ and $f_{s,\min}$):

$$V_{Cr} = X_{Cr} I_r = \frac{I_r}{\omega_s C_r} = \frac{8.1}{2\pi \cdot 55.55 \times 10^3 \cdot 97.3463 \times 10^{-9}} \approx 236.60 \text{ V}$$

RMS voltage across the resonant capacitor,

$$V_{Cr,\text{RMS}} = \sqrt{\left(\frac{V_{in,\max}}{2}\right)^2 + V_{Cr}^2} \approx 313.06 \text{ V}$$

Peak voltage corresponding to rated current,

$$V_{Cr,\text{peak}} = \frac{V_{in,\max}}{2} + \sqrt{2} V_{Cr} \approx 539.61 \text{ V}$$

Note: Metallized polypropylene film capacitors are recommended for low dissipation and high AC current capability.

9. Selection of Primary-side MOSFETs

Peak voltage across each MOSFET (off-state):

$$V_{Q1,\text{peak}} = V_{Q2,\text{peak}} = V_{in,\text{peak}} = 410 \text{ V}$$

Rated RMS current through each MOSFET:

$$I_{Q1,\text{RMS}} = I_{Q2,\text{RMS}} = 8.1 \text{ A}$$

Selection guideline: choose MOSFETs with voltage rating $> 500 \text{ V}$ and current rating $> 10 \text{ A}$ (to give margin for switching transients and thermal stress).

10. Calculation of Dead Time for ZVS Operation

It is necessary to have adequate inductive energy and sufficient dead time for zero voltage switching (ZVS). The minimum magnetizing current that occurs at the maximum switching frequency should be considered for design purposes. Additionally, for a MOSFET with a rating of 500 V, the C_{ds} is typically around 200 pF.

Minimum magnetizing current at maximum switching frequency:

$$I_{m,\min} = \frac{N_1}{N_2} \cdot \frac{V_{o,\min}}{2\pi f_{s,\max} L_m} = 1.885 \text{ A}$$

Verify energy condition by Eq.1.28 (to ensure sufficient inductive energy to discharge C_{eq} and achieve ZVS):

$$\frac{1}{2}(L_m + L_r)I_{m,peak}^2 \geq \frac{1}{2}(2C_{eq})V_{dc}^2$$

$$231.4 * 10^{-6}\text{Joule} \geq 67.24 * 10^{-6}\text{Joule}$$

Dead-time lower bound (approximate design inequality):

$$t_{\text{dead}} \geq 16 C_{eq} f_{sw} L_m$$

Using $C_{eq} \approx 400 \text{ pF}$, $f_{sw} = 149.99 \text{ kHz}$ and $L_m = 104.2 \mu\text{H}$ gives:

$$t_{\text{dead}} \geq 100 \text{ ns}$$

Therefore, a dead time more than 100 nsec is required to meet the ZVS condition.

11. Selection of Rectifier Diodes

At resonance the blocking voltage on the non-conducting diode is:

$$V_{DR2} = \frac{V_{in,\max}}{2 \cdot n} \cdot 2 \approx 82 \text{ V} \quad (2.18)$$

so select diodes with blocking rating $> 82 \text{ V}$ (preferably with margin). Average diode current:

$$I_{s,\text{av}} = \frac{\sqrt{2} I_{s1}}{\pi} \approx 12.5 \text{ A} \quad (2.19)$$

Recommendation: use fast/recovery or synchronous rectifier devices rated for the computed current and with adequate transient dv/dt and surge capability.

12. Selection of Output filter Capacitor

Such that the rectifier full wave output current is,

$$I'_o - \frac{\pi}{2\sqrt{2}} * I_o$$

For I_o , at resonance condition the capacitor's rms current is,

$$I_{C_o} = \sqrt{\left(\frac{\pi}{2\sqrt{2}} I_o\right)^2 - I_o^2} = 12.05 \text{ A}$$

A single capacitor might not be able to handle this much current, so multiple capacitors connecting in parallel are mostly used.

Chapter 3

Conclusion and Future Work

3.1 Conclusion

This report presents an overview of the LLC resonant converter, emphasizing its modeling through the Fundamental Harmonic Approximation (FHA) method and the derivation of its voltage gain expression. The LLC half-bridge converter is simulated using PLECS software, and the voltage and current waveforms under different operating modes are obtained and analyzed. Additionally, the paper examines the boundary conditions for zero-voltage switching (ZVS) and zero-current switching (ZCS), identifying the specific frequency range where ZVS is achieved. The design considerations of the converter under various operating conditions are also discussed.

3.2 Future Work

- Design and build a hardware charger for an electric vehicle rated at 1 kW, delivering 48 V output voltage, using an LLC half-bridge topology.
- The objective is to optimize the design for higher efficiency and identify the operating frequency range, series resonant component values, and transformer turns ratio at which the model achieves peak performance.
- Additionally, a control strategy will be developed to regulate the charging process within the specified voltage and current range.

References

- [1] R. W. Erickson and D. Maksimović, Fundamentals of Power Electronics Third Edition. 2020.
- [2] H. Huang, “Texas instruments power supply design seminar sem1900, topic 3 ti literature number,” 2010.

References